Libyan Journal of Veterinary and Medical Sciences (2025), Vol. 6(1): 1-6
ISSN: 🕮 2410-9215 | 💻 3080-7069

DOI: https://doi.org/10.5281/zenodo.15569964

Research article

Effect of *In-vitro* Loading on Equine Carpi of Different Morphology: A Pilot Study

Aiman H. Oheida[1]*, Abdulrhman M. Alrtib[1], Jonathan S. Merritt[2] and Helen M. S. Davies[2]

[1]*Department of Anatomy, Histology and Embryology, Faculty of Veterinary Medicine, University of Tripoli, Tripoli, Libya*
[2]*Department of Veterinary BioSciences, The University of Melbourne, Parkville, Australia*

Submitted: 21/03/2025 Accepted: 13/04/2025 Published: 16/04/2025

Abstract
Equine carpal morphology is fundamental when considering the joint stability and soundness. Although specific preferable and poor carpal conformations have been identified, it is as yet unclear how such varied carpal conformations respond to loading. This pilot study aimed to investigate the effects of in-vitro loading on carpal joints that had different bone conformations. Two carpi were selected; a carpus of a Warmblood horse (H1) with a favourable carpal conformation and a carpus of a Thoroughbred (H2) with a morphology associated with carpal pathology. Specimens were subjected to mechanical loading via an Instron test machine and dorsopalmar radiographs were taken before and after loading. Five carpal angular parameters were measured on the radiographs to assess changes in the morphometry of the carpi. The results indicated that H2 experienced greater changes in angular values, particularly in the angle of the radial facet of the third carpal bone (Rf.C3-Prx.Mc3), and instability under load. Conversely, H1 demonstrated a consistent stability, with minimal changes in the measured angles. The findings emphasize the important role of specific carpal morphology especially the angle of the radial facet of the third carpal bone in the joint stability which may be important in minimizing the risk of injury during high-speed racing.

Keywords: equine, carpus, radiology, loading, morphology

Introduction

The shape of articular surfaces might provide important information about the biomechanical action of the equine carpal joint. Detection of the load distribution through the skeleton was a principal requirement to interpret the mechanical influence of bone shape in terms of the resistance to loading (Biewener *et al.,* 1983). It might also be helpful in determining reasons for specific pathology or even help in preventing injuries. Thus, human orthopedic and biomechanical studies have paid considerable attention to the correlation between bone shape and loading in most of the skeletal bony components including the carpus (Tang *et al.,* 2013; Kim *et al.,* 2016). However, in the Veterinary field and particularly the equine carpus there have been few studies that assessed the influence of carpal bone morphology on the applied loads. Most of these studies, such as Colahan *et al.* (1987) and Palmer *et al.* (1994), concentrated mainly on the effect of increasing the load on the contact area of the carpal bones, especially on the radial facet of the third carpal bone (Rf-C3) and the force distribution through the joint.

Variation in carpal bone morphology has been found to be associated with carpal pathology in racing Thoroughbreds (Oheida *et al.,* 2022). That study identified specific anatomical features that were correlated with a higher susceptibility to injury. Such poor carpal conformation seemed to be the reasons for alterations in the loads through the carpus (Bramlage 1983; Anastasiou *et al.,* 2003). This was suggested to occur during high-speed racing where the axial load on the carpal joint was driven more towards the dorsal margins of the bones resulting in joint hyperextension with the possibility of injury (Auer, 1980; Palmer, 1986). Although equine carpal morphometery (Oheida *et al.,* 2016) and its relation to the incidence of pathology (Oheida *et al.,* 2022) have been documented, the potential alteration in different carpal conformations during loading has not been investigated. Therefore, the current experiment was designed as a pilot study to investigate the relationship between different carpal morphometries and the load transmission in an in-vitro environment. It was hypothesized that the carpus with a normal conformation would be more stable than the carpus with a conformation associated with carpal pathology during loading.

Materials and Methods

Animals

Two right forelimbs were collected from horses that were euthanized for reasons not related to their musculoskeletal systems. They were a Warmblood horse (H1) and a Thoroughbred (H2). Both selected horses were adults to avoid any effects of the radial growth plate on the results. The specimens were collected from the Pathology department of The Faculty of Veterinary Science of the University of Melbourne. The carpal joints were intact and free of any pathology.

The two specimens were specifically selected based on their morphometrical measurements (Table 1). H1 represented the favourable carpal conformation whereas

***Corresponding Author:** Aiman H. Oheida. Department of Anatomy, Histology and Embryology, Faculty of Veterinary Medicine, University of Tripoli, Tripoli, Libya. Email: a.oheida@uot.edu.ly

Table 1: Radiographic measurements of the carpal parameters in unloaded and loaded carpi

Horse	Loading	Carpal parameters				
		Ra.meta-Prx.Mc3 angle	RCJ-Prx.Mc3 angle	Rf.C3-Prx.Mc3 angle	Ra.meta-Rf.C3 angle	RCJ-Rf.C3 angle
H1	Unloaded	186.45°	183.64°	172.90°	193.55°	190.74°
	Loaded	185.79°	182.99°	172.40°	193.39°	190.59°
	Differ	0.66°	0.65°	0.50°	0.16°	0.15°
H2	Unloaded	183.37°	182.29°	175.23°	188.14°	187.06°
	Loaded	182.01°	180.94°	173.45°	188.56°	187.49°
	Differ	1.36°	1.35°	1.78°	-0.42°	-0.43°

Differ: Difference between values of angles of unloaded and loaded carpi

H2 showed the carpal conformation that was associated with a high susceptibility to damage in fast speed racing (Oheida *et al.*, 2022).

Embedding specimens

Each limb was transected through the shafts of the radius and the metacarpal bones at approximately 15 - 20 cm proximal and distal to the carpal joint. Skin and soft tissues were removed except around the carpal joint in order to keep the joint completely intact. The joint was held in an extended position by tying a thread around the radius and metacarpal bones and then positioning it in a perpendicular position, similar to the normal standing posture, using a bench clamp and clamp-stand. The ends of the metacarpal bones were embedded first in an aluminium cup and positioned perpendicular to the ground while avoiding any contact between the bone and the cup's wall. Epoxy resin and hardener (West system epoxy resin 105 and fast hardener 205, ATL Composites Pty Ltd, Ernest, Queensland, Australia) were mixed and poured into the cup and left for approximately 6 to 8 hours. The specimen was up-ended and the same procedure with a second cup was used for embedding the end of the radius (Figure 1) care was taken to ensure the bases of the two cups were maintained parallel to each other and that the specimen was perpendicular to them while the epoxy was hardening.

Installing and loading specimens

A load plate was designed to have two attached parts, upper and lower parts (Figure 1). The upper part had rounded hollows (points) which were arranged in evenly spaced lines, for receiving the loading ball of a load cell mount. There were 11 lines and each line had 11 points (Figure 2). The lower part of the load plate was made to be fixed with the cup which contained the embedded radius. The base plate consisted of two attached parts, an upper part and a base part (Figure 1). The upper part was screwed into the cup which contained the metacarpal bones. The base part was fixed on the sliding rail guides of an Instron test machine (Instron, 8874 Axial-Torsion Fatigue Testing System) thus allowing movement of the distal end of the specimen craniocaudally and providing the opportunity for the carpal joint to hyperextend.

The load cell mount was designed to be attached to the Instron test machine for loading the carpi in specific positions by placing the loading point of the Instron test machine on the loading plate. The cup with the radius was fastened to the loading plate with the dorsal/cranial surface of the specimen facing the front. The other cup with the metacarpal bones was attached to the base plate which was then fastened into the sliding rail guides of the Instron test machine. The loading ball of the load cell mount was placed on the first point of the middle line of the caudal/palmar/back edge of the loading plate (Figure 2). The thread tied at the carpus was then cut and removed.

Each specimen was loaded sequentially through two cycles. In each cycle, a vertical load was applied separately onto each of the sixth to eleventh points of the 6th line of the loading plate counting from the palmar/back edge. The load started on point six and then was moved on to the other front five points in sequence. This vertical load and the vertical displacement were recorded by the machine. The maximum peak load was approximately 2kN. The peak displacement was approximately 3mm, and displacement was applied at a rate of 1mm/s. The resultant movement in the joint was called passive moment. The data was collected using Scilab software and analysed by Scala software to measure the passive moment (N.m).

Radiography and parameters

The unloaded and loaded carpi were radiographed using the method described in Oheida *et al.* (2016). The dorsopalmar (DP) radiographs of the loaded carpi were taken while the loading point of the load cell mount was applied to the first point of the loading plate at which the carpi were in the most hyperextended position. The radiographs were entered into the EponaTech Metron software and five radiographic parameters (Oheida *et al.*, 2016) were selected and measured. The selection was made based on the clinical relevance and the potential mechanical importance of their features of interest. They focused on three relationships:

1. Effect of loading on the distal radius in relation to the proximal surface of Mc3. The selected angles were:
- Radial metaphyseal-Proximal third metacarpal angle (Ra.met-Prx.Mc3 angle)
- Radial carpal joint-Proximal third metacarpal angle (RCJ-Prx.Mc3 angle)
2. Effect of loading on the radial facet of C3 in relation to the proximal surface of Mc3. The angle was:
- Radial facet C3-Proximal third metacarpal angle (Rf.C3-Prx.Mc3 angle)
3. Effect of loading on the distal radius in relation to the radial facet of C3. The angles were:
- Radial metaphyseal-Radial facet C3 angle (Ra.met-Rf.C3 angle)

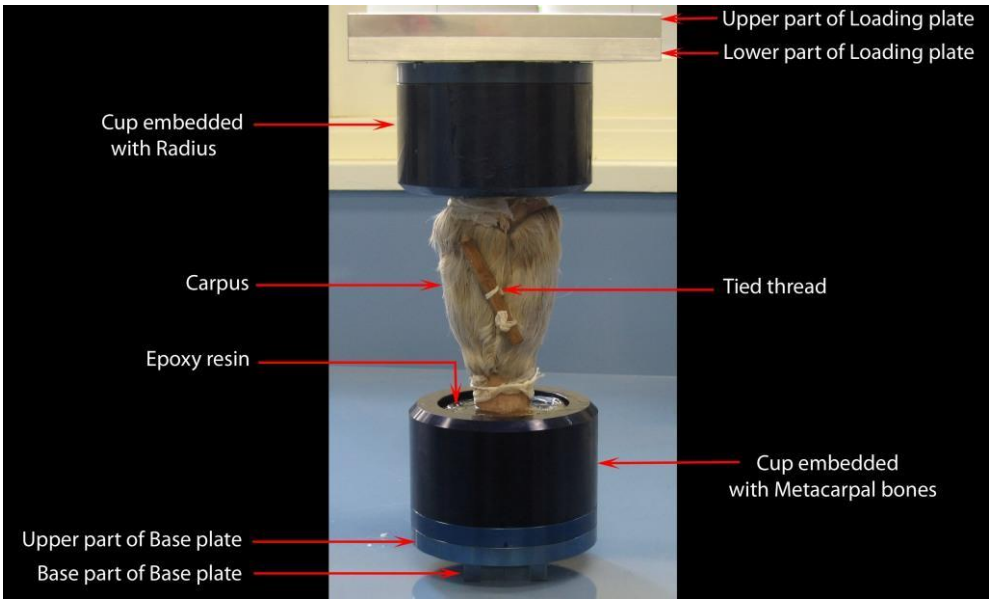

Figure 1. A right carpus embedded into two cups. The first cup with the metacarpal bones was screwed into the upper part of the base plate. The second cup with the radius was attached to the lower part of the loading plate. A thread was tied at the dorsal aspect of the carpus. Both the cups were filled with epoxy resin.

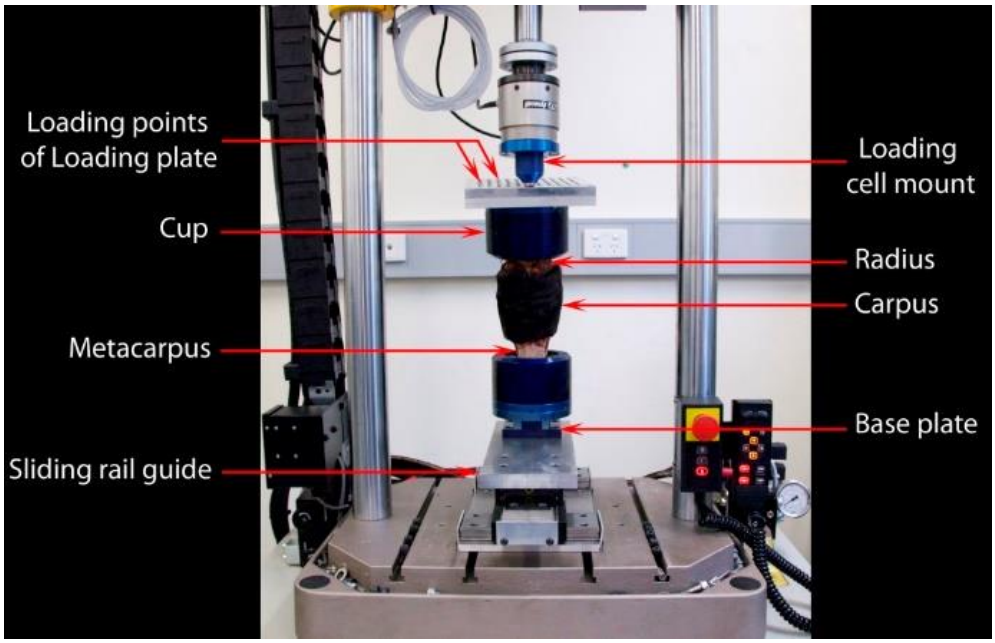

Figure 2. Dorsal aspect of the embedded carpus that was loaded inside the Instron test machine. The load cell mount was placed on the loading plate. The base plate was fixed into the sliding rail guide of the base of the machine.

- Radial carpal joint-Radial facet C3 (RCJ-Rf.C3 angle)

All the radiographic measurements were conducted by the first author to minimize the variation between measurements (Kublashvili *et al.*, 2004).

Measuring the joint hyperextension

The embedded carpi were photographed from the side (perpendicular to the direction of movement) using a fixed camera during the loading and unloading phases. The photographs were used to locate the centre of carpal joint rotation and measure the degree of hyperextension.

Ethical approval

As the experimental work was conducted on cadavers from horses that died for reasons not associated with the experiment, no ethical approval was required.

Results

Generally, the H2 carpus showed a larger change in the values of the five angles than the H1 carpus. Despite increasing or decreasing the values, the measurements demonstrated that the Rf.C3-Prx.Mc3 angle of H2 was the most affected angle during loading. It changed from 175.23° when unloaded to 173.45° in the loaded joint.

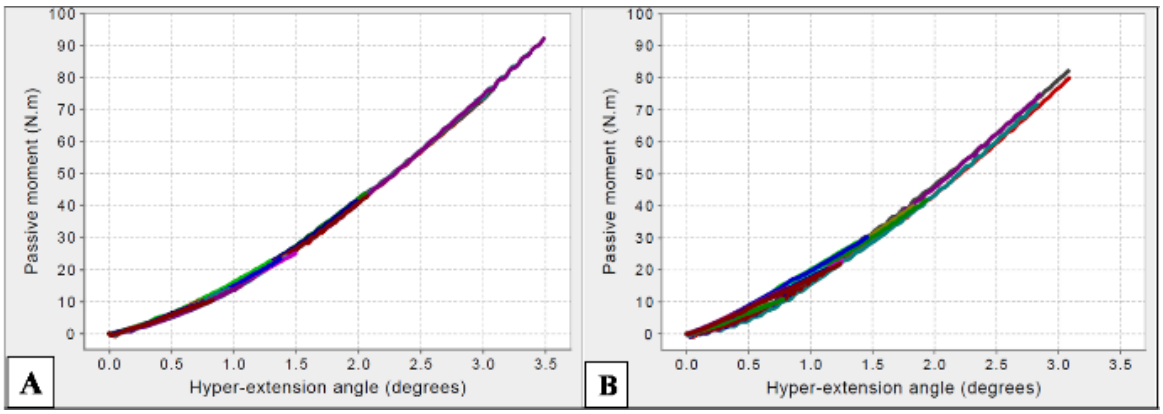

Figure 3. Angular stiffness of Horse 1 (A) and Horse 2 (B) during loading of their embedded carpi. These showed the relatively consistent relationship between increasing the hyperextended carpal angle and the passive moment (N.m) in the two horses. There was more variation and lack of fit between the different runs in H2 (B).

In addition, it was noted that there was a decrease in the values of the parameters when the carpi were loaded (Table 1) except in the Ra.met-Rf.C3 angle and the RCJ-Rf.C3 angle of H2 which showed a small increase of less than 0.45° in their values. The measurements within each horse revealed that the minimum changes were seen in the Ra.met-Rf.C3 angle and RCJ-Rf.C3 angle.

Applying the load on the embedded carpi resulted in an increase of both the hyperextension carpal angle and the passive moment. This linear relationship was represented clearly in both the specimens. However, although H1 showed stability in this relationship through loading at the different loading points (Figure 3.A), H2 showed avariable response to the load with less fit between the slopes from the different loading points (Figure 3.B).

Discussion

Although carpal morphology is believed to be an important factor in relation to equine carpal soundness and pathology, effects of loading of carpi of varying conformations on the joint stability has not been investigated. The current pilot study provided some initial evidence about the different response to in-vitro loads of equine carpi with specific variations in morphology.

The radiographic measurements of the two specimens revealed that all the changes in the measured angles were greater in H2 than in H1. The Rf.C3-Prx.Mc3 angle of H2 was the most affected parameter by the loads. The amount of change in the measurements between the unloaded and loaded carpus was 1.78°. In terms of affecting the load on the relationships between the bony components of this angle, the alteration could indicate that the slope of the radial facet of C3 in relation to the proximal articular surface of Mc3 would be more affected by loading when they have the conformation previously related to early career carpal injury (Oheida *et al.*, 2022). It is difficult to recognize whether the radial facet of C3 or the proximal Mc3 was the main reason for such an influence. Angulation of the proximal Mc3 is less likely to be the cause because the locations of its medial and lateral landmarks were found to be invariable and the line formed between them was more parallel to the ground (Abdunnabi, 2011). Whereas, decreasing the distomedial slope of the radial facet of C3 in H2 might not be helpful in dissipating some of the axial load to the adjacent medial soft tissues (Oheida *et al.*, 2022). If so, then what might be the effect of the tremendous loads, which could be up to 9kN (Palmer *et al.*, 1994), experienced on a poorly conformed carpus during fast racing in contrast to the 2kN maximum load applied in this pilot study?

Based on the differences in the measurements between loaded and unloaded carpus in each specimen, it was noticed that the Ra.met-Rf.C3 and RCJ-Rf.C3 angles demonstrated the minimum amount of changes compared to the other three angles. This was very obvious in H1 with the favoured morphology in which the RCJ-Rf.C3 angle showed a minor change of 0.15°. Accordingly, the current finding would mean that the angulation of the distal radius in relation to the radial facet of C3 is probably more consistent during load transmission. Even with this supposition, the increase in the values of the two angles in H2 put more doubt about the ability of such a conformation to provide joint stability. Pathologically, the distal radius and the radial facet of C3 were the most injured parts of the carpus in racehorses (McIlwraith *et al.*, 1987; Garvican and Clegg, 2007). Oheida *et al.* (2022) reported a significant negative correlation between the angulation in the distal radius-radial facet of C3 and the incidence of carpal pathology. The less angled this part of C3 the more likely the damage. Hence, an explanation for how highly damaged features showed more constant relationships during loading seems to be more complicated. However, it might be assumed that the inability of the radial facet of C3 to dissipate the entire received load to soft tissues (Bramlage *et al.*, 1988; Pagliara *et al.*, 2022) participated in minimising the changes of its relationship to the proximally located radius. The biomechanical function of the radial facet of C3 whether in relation to the radius or to the large metacarpal bone requires more investigation.

Measuring the hyperextension of the carpal angle and the passive moment in relation to the loading revealed not only the consistent relationship between the carpal hyperextension and the passive moment but also some differences in the pattern of the response in H1 and H2 to the loads. Interestingly, the response of the H1 carpus was consistent and regular throughout the different

loading runs (Figure 3.A) with a slightly greater hyperextension. Whereas, the H2 carpus showed some instability and lack of fit in the response to load between the different loading runs (Figure 3.B). This finding, and in addition to the above discussed radiographic results, suggests that applying the load to a carpus which has a preferable conformation leads to more joint stability. Further, carpal joint hyperextension is thought to be one of the most common reasons for carpal damage (Park *et al.*, 1970; Auer, 1980). In this study however, the slight carpal hyperextension seems to have had no effect on the joint stability as long as the joint had a superior conformation. There is a belief that the geometrical properties of the articular surfaces determine the stability of their joints (Sledge, 1993). This should have more attention in loading the equine carpal joint in which the applied load was transmitted more through its contacted articular surfaces than through the soft tissues and subchondral bone (Palmer and Bertone, 1996) especially in the medial aspect of the middle carpal joint (Pagliara *et al.*, 2022). At this important region, the load passes from radius to radial carpal bone then is entirely received on the concave radial facet of C3 without any attenuation (Bramlage *et al.*, 1988). Hence the joint stability will be questionable when the carpal conformation was poor particularly in the radial facet of C3 in relation to the distal radius and proximal Mc3 as seen in H2.

The results of testing the load in only two carpi in this experiment are obviously insufficient to verify the relationship between carpal conformation and the stability of the loaded joint. However, it may promote a more extensive experiment using the same methodology. The carpi should be categorized into three groups based on their morphometrical measurements of the significant features; carpi with the highest, around the average and with the lowest morphometrical values as described in Oheida *et al.* (2022). Applying loads on these carpal groups seems likely to provide satisfactory evidence about the mechanical effect of the varied carpal morphology on the stability of the loaded joint.

Conclusion

This pilot study showed various responses of two carpal joints with different conformation to in-vitro loading. The carpus with the favourable carpal morphometry appeared more stable during loading than the carpus with conformation previously associated with carpal damage. Angulation of the radial facet of C3 seemed to have a fundamental mechanical role in loading the joint. As the results in this study were derived from applying only in-vitro loads of a maximum 2kN, well below the 9kN that this joint is thought to withstand, further investigations are required to evaluate the mechanical effect of carpal morphology on the stability of the loaded joint in racehorses.

Conflict of interest

The authors declare no conflicts of interest in relation to this work.

Authors' contribution

Oheida A.H.: Study conception and design, writing the manuscript; Alrtib A.M.: Experimental design and revision of the manuscript; Merritt J.S.: Loading design and analysis; Davies H.M.S.: Supervision of the experiment and revision of the manuscript. All authors contributed in performing the experimental work.

Acknowledgment

The authors would like to thank Brendan Kehoe, Hossein Mokhtarzadeh and Prof. Peter Lee for their assistance.

References

Abdunnabi, A. H. S. (2011). *Morphometry of the equine carpus and its relationship to carpal bone pathology* (Doctoral dissertation, University of Melbourne, Department of Veterinary Science).

Anastasiou, A., Skioldebrand, E., Ekman, S., & Hall, L. D. (2003). Ex vivo magnetic resonance imaging of the distal row of equine carpal bones: assessment of bone sclerosis and cartilage damage. *Veterinary Radiology & Ultrasound*, *44*(5), 501-512.

Auer, J. (1980). Diseases of the carpus. *The Veterinary Clinics of North America. Large Animal Practice*, *2*(1), 81-99.

Biewener, A. A., Thomason, J., & Lanyon, L. E. (1983). Mechanics of locomotion and jumping in the forelimb of the horse (Equus): in vivo stress developed in the radius and metacarpus. *Journal of Zoology*, *201*(1), 67-82.

Bramlage, L. R. (1983). Surgical diseases of the carpus. Vet Clin North Am Large Anim Pract 5:261-274.

Colahan P, Turner, T., Poulos, P., Piotrowski, G. (1987). Mechanical function and sources of injury in the carpus and fetlock. Proc Am Ass Equine Practnr 33:689-699.

Garvican, E., & Clegg, P. (2007). Clinical aspects of the equine carpal joints. *UK Vet Companion Animal*, *12*(1), 5-12.

Kim, B. J., Kovacevic, D., Lee, Y. M., Seol, J. H., & Kim, M. S. (2016). The role of lunate morphology on scapholunate instability and fracture location in patients treated for scaphoid nonunion. *Clinics in Orthopedic Surgery*, *8*(2), 175-180.

Kublashvili, T., Kula, K., Glaros, A., Hardman, P., & Kula, T. (2004, September). A comparison of conventional and digital radiographic methods and cephalometric analysis software: II. Soft tissue. In *Seminars in Orthodontics* (Vol. 10, No. 3, pp. 212-219). WB Saunders.

McIlwraith, C. W., Yovich, J. V., & Martin, G. S. (1987). Arthroscopic surgery for the treatment of osteochondral chip fractures in the equine carpus. *Journal of the American Veterinary Medical Association*, *191*(5), 531-540.

Oheida, A. H., Alrtib, A. M., Abushhiwa, M. H., Philip, C. J., & Davies, H. (2022). Carpal Morphometry in Normal Horses and Horses with Carpal Bone Pathology. *Alexandria Journal of Veterinary Sciences*, *72*(1), 1-8.

Oheida, A. H., Anderson, G. A., Alrtib, A. M., Abushhiwa, M. H., Philip, S., & Davies, H. M. S. (2016). Carpal parameters on dorsopalmar radiographs of the equine carpus. *Journal of Veterinary Advances*, *6*(6), 1258.

Pagliara, E., Pasinato, A., Valazza, A., Riccio, B., Cantatore, F., Terzini, M., & Bertuglia, A. (2022).

Multibody computer model of the entire equine forelimb simulates forces causing catastrophic fractures of the carpus during a traditional race. Animals, 12(6), 737.

Palmer, J. L., Bertone, A. L., & Litsky, A. S. (1994). Contact area and pressure distribution changes of the equine third carpal bone during loading. Equine veterinary journal, 26(3), 197-202.

Palmer, J. L., & Bertone, A. L. (1996). Joint biomechanics in the pathogenesis of traumatic arthritis. Joint disease in the horse, 104-119.

Palmer, S. E. (1986). Prevalence of carpal fractures in Thoroughbred and Standardbred racehorses. Journal of the American Veterinary Medical Association, 188(10), 1171-1173.

Park, R. D., Morgan, J. P., & O'Brien, T. (1970). Chip fractures in the carpus of the horse: a radiographic study of their incidence and location. Journal of the American Veterinary Medical Association, 157, 1305-1312.

Sledge C. (1993). Biology of the joint. In: Textbook of Rhenumatology. Ed: Kelley WN, Harris ED, Ruddy S, Sledge CB. Philadelphia, WB Saunders 1-21.

Tang, P., Swart, E., Konopka, G., Raskolnikov, D., &Katcherian, C. (2013). Effect of capitate morphology on contact biomechanics after proximal row carpectomy. The Journal of Hand Surgery, 38(7), 1340-1345.